Transition radiation

L. Fayard

TRANSITION RADIATION

L. Fayard

Laboratoire de l'Accélérateur Linéaire, Bât. 200, F-91405 Orsay Cedex, France

Résumé : Le principe du rayonnement de transition est décrit. On montre des applications dans le domaine du visible et dans les rayons X.

Abstract : The principles of Transition-Radiation are described. Some applications of Optical and X-ray Transition Radiation are shown.

I - INTRODUCTION

A radiation is produced when a charged particle passes through the interface between two media having different dielectric properties. This radiation -*Transition radiation* - has been predicted in 1944 by V. Ginzburg and I. Frank[1]. It is produced in transmission *and* in reflection. It has been observed for the first time in 1959 by Goldsmith and Jelley[2]. The radiation produced in reflection by 1 - 5 MeV (kinetic energy) protons entering a metal surface was detected in the optical range.
In 1959 Garibyan[3] and Barsukov[4] showed that for relativistic particles the total intensity of the radiation (integrated over all angles and frequencies) produced in transmission on an interface is proportional to $\gamma = E/m$. This opened up wider perspectives for the creation of "transition counters" used for determination of relativistic particle energies. It was suggested in 1958[5] to add the radiations of several interfaces. The proportionality to γ of the intensity was then measured in 1970[6]. In the mid 70's transition radiation started to be used also for beam diagnostics[7].

II - GENERAL FORMULAS AND PROPERTIES OF TRANSITION RADIATION

For detailed computations the reader should consult references[8-11].

II.1 - General formula for normal incidence

Let us consider the radiation produced by a unit charge particle of velocity $\vec{v} = \vec{\beta}c$ going from medium 1 (with permittivity ϵ_1) to medium 2 (ϵ_2). The differential intensity I1 in reflection is given by :

$$\frac{dI_1}{d\Omega\, d\hbar\omega} = \alpha\beta^2 \frac{\sqrt{\epsilon_1}}{\pi^2} \sin^2\theta_1 \cos^2\theta_1 \times \left| \frac{(\epsilon_2 - \epsilon_1)\left(1-\beta^2\epsilon_1 + \beta\sqrt{\epsilon_2 - \epsilon_1 \sin^2\theta_1}\right)}{\left(1-\beta^2\epsilon_1\cos^2\theta_1\right)\left(1+\beta\sqrt{\epsilon_2 - \epsilon_1\sin^2\theta_1}\right)\left(\epsilon_2\cos\theta_1 + \sqrt{\epsilon_1\epsilon_2 - \epsilon_1^2\sin^2\theta_1}\right)} \right|^2 \quad (2.1)$$

where θ_1 (see figure 1) is between 0 and $\pi/2$. The differential energy in transmission $dI_2/d\Omega.d\hbar\omega$ is given (for θ_2 between 0 and $\pi/2$) by the same formula *with* $\theta_1 \to \theta_2$, $\epsilon_1 \Leftrightarrow \epsilon_2$, $\beta \to -\beta$. The

polarisation of the radiation is parallel to the observation plane (plane defined by the normal to the interface and $\vec{n}$. Finally we note that this formula is deduced using *classical* electrodynamics and that we have done $\mu_1 = \mu_2 = 1$.

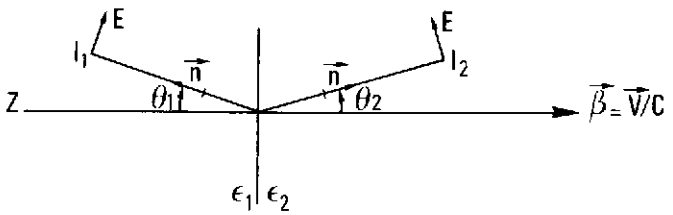

Fig. 1 - Crossing a boundary of two media by a unit charge

II.2 - Formulas for oblique incidence

They are more complicated. They can be found in ref [8, 11, 12]. A notable difference is that parallel and perpendicular polarisations are present in this case.

II.3 - Transition vacuum-medium. Physical interpretation

Let us consider (fig. 2) a particle going at normal incidence from a medium ($\epsilon_1 = \epsilon$) to the vacuum ($\epsilon_2 = 1$). We have, from (2.1)

$$\frac{dI_2}{d\Omega d\hbar\omega} = \frac{\alpha\beta^2 \sin^2\theta \cos^2\theta}{\pi^2\left(1-\beta^2\cos^2\theta\right)^2} \left| \frac{(\epsilon-1)\left(1-\beta^2 - \beta\sqrt{\epsilon - \sin^2\theta}\right)}{\left(\epsilon\cos\theta + \sqrt{\epsilon - \sin^2\theta}\right)\left(1-\beta\sqrt{\epsilon - \sin^2\theta}\right)} \right|^2 \qquad (2.2)$$

which is equal to :

$$\frac{dI_2}{d\Omega d\hbar\omega} = \frac{\alpha^2\beta^2}{4\pi^2} \sin^2\theta \left| \frac{1}{1-\beta\cos\theta} + \frac{r''}{1+\beta\cos\theta} - \frac{f''}{\sqrt{\epsilon}} \frac{1}{1-\beta\sqrt{\epsilon - \sin^2\theta}} \right|^2 \qquad (2.3)$$

$$= \frac{\alpha^2\beta^2}{4\pi^2} \sin^2\theta \left|D + R + T\right|^2$$

where $r'' = (\epsilon \cos\theta - \sqrt{\epsilon - \sin^2\theta}) / (\epsilon\cos\theta + \sqrt{\epsilon - \sin^2\theta})$ and $f'' = (1 + r'')/\sqrt{\epsilon}$ are the reflection and refraction Fresnel coefficients [13, 14] for parallel polarisation. We see that the intensity is given by the sum of the three waves D, R and T. We can note that the pole of T includes Cerenkov radiation (when $\beta n > 1$). This pole corresponds to $1 - \beta\sqrt{\epsilon - \sin^2\theta} = 0 = 1 - \beta\sqrt{\epsilon}\sqrt{1 - \sin^2\theta'}$ which gives $\cos\theta' = \frac{1}{\beta\sqrt{\epsilon}} = \frac{1}{\beta n}$, the usual Cerenkov formula.

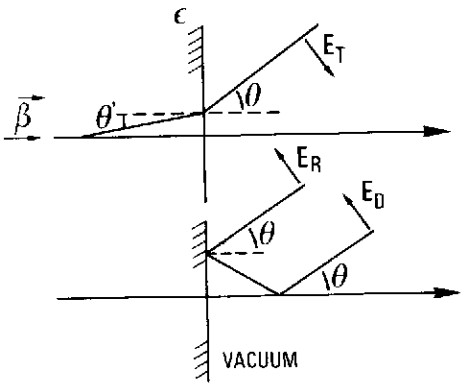

Fig. 2 - Field generated by a particle crossing a boundary of two media

II.4 - Non relativistic limit

In the case of normal incidence of a particle going from the vacuum to a medium the intensity detected in the vacuum at an angle θ (fig. 3a) is given by

$$dI_1 / d\Omega d\hbar\omega = (\alpha\, \beta^2 \sin^2\theta / \pi)\ .\ B$$

where

$$B = \left| (\epsilon - 1)\cos\theta / (\epsilon \cos\theta + \sqrt{\epsilon - \sin^2\theta}\ ) \right|^2 .$$

For a perfect conductor ($\epsilon \to \infty$) B is equal to 1. For an oblique incidence we have $dI_1 / d\Omega d\hbar\omega = (\alpha\, \beta_z^2 \sin^2\theta / \pi)$.B where β_z is the component of $\vec{\beta}$ along the normal $\hat{z}$. We can note that in all cases the field $\vec{E}$ is in the plane ($\hat{z}$, $\vec{\beta}$). This polarisation property was used already in the original work of Goldsmith and Jelley[2].

II.5 - Length of the formation zone

The concept of the radiation formation zone and its size L_f are of great importance for transition radiation[15, 16]. Let us consider (fig. 3b) a particle moving at velocity $\vec{v} = \vec{\beta}\ c$ in a medium with refractive index $n = \sqrt{\epsilon}$ and emitting waves at angle θ. Let at the moment t = 0 the source be at a point A and the phase of the wave emitted by it in direction $\vec{k}$ be equal to ϕ_A. We define the formation time t_f as the time after which the phase of the wave ϕ_B emitted at a point B in the same direction $\vec{k}$ differs from the phase of the wave ϕ_A emitted at point A by 2π. The phase factor of the wave has the form exp iφ = exp i ($\vec{k}\,\vec{r} - \omega t$). As it is clear from figure 3b.

$$|\phi_A - \phi_B| = |kL_f \cos\theta - \omega t_f| = \left|\frac{\omega n}{c} v t_f \cos\theta - \omega t_f\right| \qquad (2.4)$$

since the size of the formation zone is $L_f = vt_f$. It follows from (2.4) that :

$$L_f = vt_f = \frac{(v\sqrt{\epsilon}/c)\,\lambda}{|1 - (v/c)\sqrt{\epsilon}\cos\theta|} \qquad (2.5)$$

where λ is the wave length $\lambda = 2\pi c / (\sqrt{\epsilon}\,\omega)$. We see that for interesting cases ($\cos\theta \sim 1$, $\sqrt{\epsilon} \sim 1$, $v/c \sim 1$) we have $L_f \gg \lambda$.

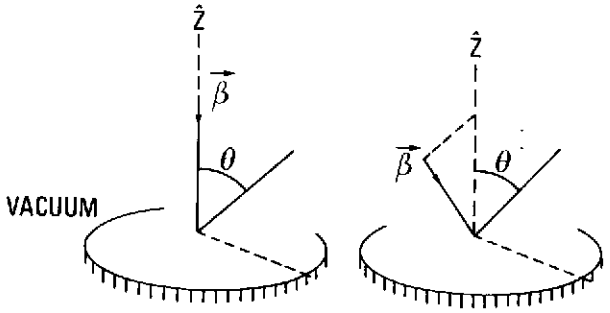

Fig. 3a - A particle going from vacuum to medium

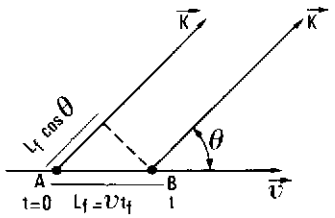

Fig. 3b - The length L_f of the radiation formation zone

II.6 - The Wartski Interferometer

The intensities I_1 and I_2 of transition radiation emitted on the two interfaces of figure 4a by a particle at normal incidence are deduced from (2.1).

$$\frac{dI_2}{d\Omega d\hbar\omega} = \frac{\alpha^2\beta^2}{4\pi^2}\sin^2\theta_2 \left| \frac{1}{1-\beta\cos\theta_2} + \frac{r''}{1+\beta\cos\theta_2} - \frac{f''}{\sqrt{\epsilon}} \frac{1}{1-\beta\sqrt{\epsilon - \sin^2\theta_2}} \right|^2 \qquad (2.6)$$

$$\frac{dI_1}{d\Omega d\hbar\omega} = \frac{\alpha^2\beta^2}{4\pi^2}\sin^2\theta_1 \left| \frac{1}{1+\beta\cos\theta_1} + \frac{r''}{1-\beta\cos\theta_1} - \frac{f''}{\sqrt{\epsilon}} \frac{1}{1+\beta\sqrt{\epsilon - \sin^2\theta_1}} \right|^2$$

If we are interested in the optical range of the spectrum (where ϵ is notably different from 1) produced by relativistic particles at small angles we have $\beta \approx 1 - 1/(2\gamma^2)$, $\cos\theta \simeq 1 - \theta^2/2$. Only the first term for dI_2 and the second term for dI_1 contributes significantly. So $dI_1 \alpha\ dI_2\ \alpha\ \theta^2/(\theta^2 + 1/\gamma^2)^2$. The total intensity dI_{TOT} sum of the radiations dI_2 (reflected on the medium ϵ) and dI_1 is different from $dI_1 + |r''|^2 dI_1$ due to the *interference* terms. We then have, setting $\theta = \theta_1 = \theta_2$.

$$\frac{dI_{TOT}}{d\Omega d\hbar\omega} \approx \frac{\alpha^2\beta^2 \sin^2\theta |r''|^2}{4\pi^2} \left(\frac{1}{1-\beta\cos\theta}\right)^2 |1 - e^{-i\varphi}|^2 \qquad (2.7)$$

where $\varphi = 2\pi L/L_f$ and $|1 - e^{-i\varphi}|^2 = 4\sin^2\varphi/2$. We have a standard study of interference fringes (see ref. 13, chap. 7) apart that the phase difference is $2\pi L/L_f$ instead of $2\pi L/\lambda$. The length of the formation zone in the vacuum L_f plays the role of the wavelength λ. The *order of interference* p is defined by $\varphi/2 = p\pi$ and p is equal to

$$p = \varphi/2\pi = L/L_f = \frac{L}{\lambda\beta}(1 - \beta\cos\theta_p) \approx \frac{L}{2\lambda}\left(\frac{1}{\gamma^2} + \theta_p^2\right) = p_o + \frac{L}{2\lambda}\theta_p^2 \text{ with } p_o = \frac{L}{2\lambda\gamma^2}$$

The angular radii of the intensity maxima (p integer) and minima (p half integer) are given by

$$\theta_p \approx \left[(2\lambda/L)\,(p - p_o)\right]^{1/2} \tag{2.8}$$

These interference fringes were first observed by Wartski and coworkers[7,11] at Saclay using an electron beam of energy between 35 and 72 MeV ($68.5 < \gamma < 140.9$). The optical transition radiation was emitted on the boundaries between vacuum and aluminium foils. The experimental arrangement was similar to figure 4b. When the particles are relativistic it can be shown that the high directivity radiation is emitted around the direction of the particle and around the direction of specular reflection. Formulas (2.7) and (2.8) are still valid for the case of figure 4b. This method can also be used in order to estimate the beam energy and the angular spread of the beam.

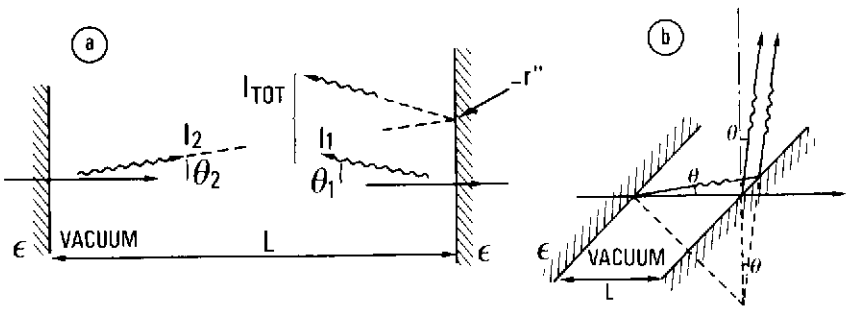

Fig. 4 - Two parallel foils

II.7 - Optical Transition Radiation Diagnostics for Beams

Transition radiation has been used in order to measure the beam profile of the CERN-SPS[17]. The small duration of the transition radiation will be used to determine the length of the short ($\tau \sim 10^{-11}$ s) electron bunches produced by the lasertron in Orsay[18, 19]. A new emphasis has been recently[20] put on measurement of emittance of electron beams.

III - SEPARATION OF RELATIVISTIC CHARGED PARTICLES

The transition radiation counter, for ultra relativistic particles with a multifoil radiator and an X-ray detector is very useful in high energy physics (see ref.[21] for example). The analysis of the parameters of such counters is then of great importance. Detailed studies can be found in ref.[8,9,14,22-27] and only the main results are presented here.

In this chapter we will consider that the frequency ω of the radiation is much larger than the Plasma frequencies ω_p of the materials where $\hbar\,\omega_p \approx 28.8\text{ eV} \times \sqrt{\frac{Z\rho}{A}}$ with ρ being the density in g cm^{-3}. In this limit it is possible to use the formula $\epsilon \approx 1 - \omega_p^2/\omega^2$.

III.1 - Comparison of Forward and Backward Radiations

Let us consider the radiations produced in the vacuum at an angle θ from the trajectory by a particle at normal incidence on a medium with a permittivity ϵ. I_1 and I_2 are the backward and forward radiations. Using (2.3) one finds :

$$\frac{dI_2}{d\Omega d\hbar\omega} = \frac{\alpha^2\beta^2}{4\pi^2}\sin^2\theta\left|\frac{1}{1-\beta\cos\theta}+\frac{r''}{1+\beta\cos\theta}-\frac{f''}{\sqrt{\epsilon}}\frac{1}{1-\beta\sqrt{\epsilon-\sin^2\theta}}\right|^2$$

$$\frac{dI_1}{d\Omega d\hbar\omega} = \frac{\alpha^2\beta^2}{4\pi^2}\sin^2\theta\left|\frac{1}{1+\beta\cos\theta}+\frac{r''}{1-\beta\cos\theta}-\frac{f''}{\sqrt{\epsilon}}\frac{1}{1+\beta\sqrt{\epsilon-\sin^2\theta}}\right|^2 \qquad (3.1)$$

These equations are similar to (2.6) but now we are interested in the X-ray part of the spectrum instead of the optical part and $\epsilon \approx 1 - \frac{\omega_p^2}{\omega^2}$ is around 1. So if dI_1 has still a significant contribution from only its second term, the first *and third term* of dI_2 contributes. This difference will explain why the main part of the energy emitted by ultrarelativistic particles is in the forward direction. The backward radiation has the approximate form :

$$\frac{dI_1}{d\Omega\hbar\omega} \approx \frac{\alpha}{\pi^2}\left(\frac{\sqrt{\epsilon}-1}{\sqrt{\epsilon}+1}\right)^2\frac{\theta^2}{(\theta^2+1/\gamma^2)^2} \qquad (3.2)$$

Integrating I_1 over angles and frequency one finds[9] $I_1 \sim (2\alpha/15\pi)\cdot\omega_p\,\ell n\,\gamma$. This total intensity has a *logarithmic* dependance on the particle energy. For the forward radiation we find :

$$\frac{dI_2}{d\Omega\hbar\omega} \approx \frac{\alpha\theta^2}{\pi^2}\left(\frac{1}{\theta^2+1/\gamma^2}-\frac{1}{\theta^2+1/\gamma^2+\omega_p^2/\omega^2}\right)^2 \qquad (3.3)$$

The distribution of $(1/I_2)\cdot dI_2/d(\gamma\theta)$ is shown on figure 5a. It can be shown that the most probable angle has the value $\theta mp \approx 1/\gamma$ and that the root-mean-squared angle has the value $\theta rms = \langle\theta^2\rangle^{1/2} \approx \left[(1/\gamma^2)+(\omega_p^2/\omega^2)\right]^{1/2}$ which may be much larger than θmp if $\omega < \gamma\omega_p$. Integrating formula (3.3) over angles one finds :

$$\frac{dI_2}{d\hbar\omega} = \frac{\alpha}{\pi}\left\{\left(1+2\frac{\omega^2}{\omega_{cr}^2}\right)\cdot\ell n\left(1+\frac{\omega_{cr}^2}{\omega^2}\right)-2\right\} \qquad (3.4)$$

where $\omega_{cr} = \gamma\omega_p$. The emitted forward energy integrated over frequencies is equal to $I_2 = \alpha\gamma\hbar\omega_p/3 = \alpha\hbar\omega_{cr}/3$. It is *proportional to the particle energy*. $dI_2/d\hbar\omega$ is shown in figure 5b for the example of a boundary vacuum-polypropylene ($\hbar\omega_p$ = 21 eV). One can see that about 90 % of the intensity is obtained for frequencies between ω_{cr} and $\omega_{cr}/100$. ω_{cr} is a *frequency cut-off*, the necessary condition for having significant yield being $\omega \le \omega_{cr}$.

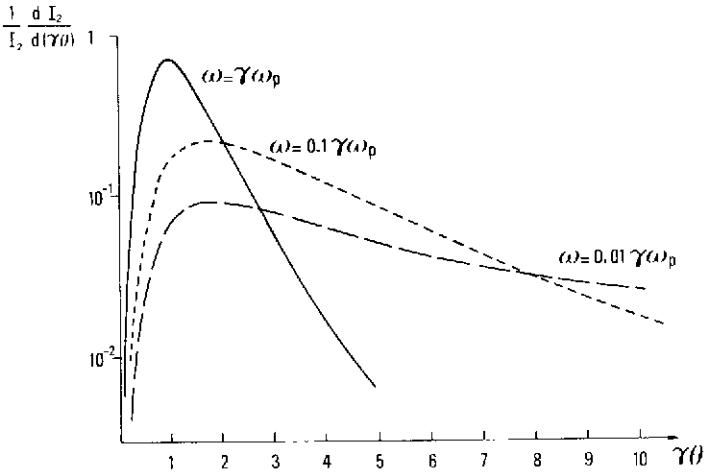

Fig. 5a - Differential distribution of the forward intensity as a function of $\gamma\theta$ for different frequencies of the radiation

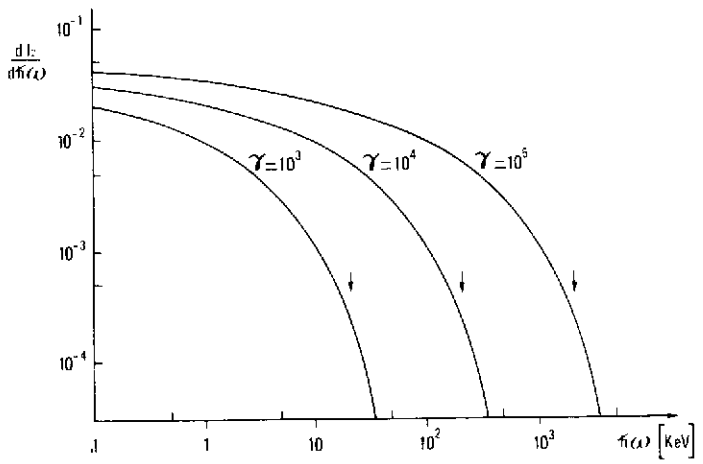

Fig. 5b - Intensity of the forward radiation at several values of γ for polypropylene ($\hbar\omega_p$ = 21eV). The arrows are at $\gamma\hbar\omega_p$

III.2 - General formulas at oblique incidence

It has been shown by Garibyan[28] that formula (3.3) holds for oblique incidence provided θ is now the angle between the radiation and the direction of the particle. If we consider a transition between 2 media with plasma frequencies ωp_1 and ωp_2 the generalisation of (3.3) is for the forward radiation.

$$\frac{dI_1}{d\Omega\hbar\omega} \approx \frac{\alpha\theta^2}{\pi^2}\left(\frac{1}{\theta^2 + 1/\gamma^2 + \omega p_2^2/\omega^2} - \frac{1}{\theta^2 + 1/\gamma^2 + \omega p_1^2/\omega^2}\right)^2 \qquad (3.5)$$

The total intensity is given by $I = (\alpha\gamma\hbar\omega p_1/3)\,.\,(1 - \omega p_2/\omega p_1)^2 / (1 + \omega p_2/\omega p_1)$. If $\omega p_2 \ll \omega p_1$, one gets :

$$\theta mp \approx \left(\frac{1}{\gamma^2} + \frac{\omega p_2^2}{\omega^2}\right)^{1/2} \text{ and } \theta rms \approx \left(\frac{1}{\gamma^2} + \frac{\omega p_1^2}{\omega^2}\right)^{1/2}$$

III.3 - Transition radiation produced by a single foil

Let us consider the case of a foil of thickness ℓ_1 (along the direction of the particle) and plasma frequency ωp_1 in a medium of plasma frequency $\omega p_2 \ll \omega p_1$. The intensity of the radiation is equal to :

$$\frac{dI}{d\Omega\hbar\omega}\,(\text{foil}) = \frac{dI}{d\Omega\hbar\omega}\,(\text{surface}) \bullet F \qquad (3.6)$$

where F is the *interference term* . If we neglect the absorption this term is equal to $|1 - e^{-\varphi_1}|^2$ where $\varphi_1 = 2\pi\ell_1/Lf_1$, Lf_1 being the length of the formation zone in the foil. But we have absorption. It means that $\epsilon_1 \approx 1 - \omega p_1^2/\omega^2$ has a *small* imaginary part which can be neglected when computing the intensity of a single surface. But it will contribute in absorbing the radiation produced at the entrance of the foil. F is then equal to $|1 - e^{-\sigma_1 - i\varphi_1}|^2 = 4\,e^{-\sigma_1}\left[\mathrm{sh}^2(\sigma_1/2) + \sin^2(\varphi_1/2)\right]$ with $\sigma_1 = \ell_1/2\,L_{A1}$, L_{A1} being the *intensity absorption length.*

If one neglects the absorption F is proportional to :

$$\sin^2(\varphi_1/2) = \sin^2\left[(\ell_1\,\omega/4)\,.\,(\theta^2 + 1/\gamma^2 + \omega p_1^2/\omega^2)\right]$$

Neglecting θ^2 and $1/\gamma^2$ in front of $\omega p_1^2/\omega^2$ one gets $\sin^2(\varphi_1/2) \approx \sin^2(\ell_1\,\omega p_1^2/4\omega)$. We have some *frequency maxima* $\bar{\omega}_n$ such that $\ell_1\,\omega p_1^2/4\bar{\omega}_n = \pi/2 + n\pi$

$$\bar{\omega}_n = \frac{\ell_1\,\omega p_1^2}{2\pi}\,\frac{1}{(1 + 2n)}\,,\ n \text{ integer} \qquad (3.7)$$

Due to absorption the important maximum is $\bar{\omega}_0$. One has an other *frequency cut-off* $\omega_c = \pi\bar{\omega}_0$ which is *independant of* γ but a function of the thickness ℓ_1 of the foil. Generally for high γ this frequency cut-off is smaller than the single foil cut-off ω_{cr}. Figure 6a shows the exact computation[22] of the differential energy spectrum produced on a single foil of polypropylene neglecting absorption. The frequencies $\bar{\omega}_n$ are clearly visible. Figure 6b shows the intensity per interface for a single interface and a single foil (still neglecting absorption). One sees for the single foil case a linear rise (I) followed by a logarithmic rise (II) for $\gamma \gg \gamma_c$ where $\gamma_c = \ell_1\,\omega_{p1}/2$ has been defined by the equation $\gamma_c\ \omega_{p1} = \omega_c$. Below γ_c the intensity of a foil is equal to twice the intensity of an interface : the average (on θ,ω) of $\sin^2\varphi_1/2$ is 1/2.

We can note finally that this "formation-zone effect" producing in particular the frequencies $\bar{\omega}_n$ has been seen in the X-ray domain by several experiments[26,29].

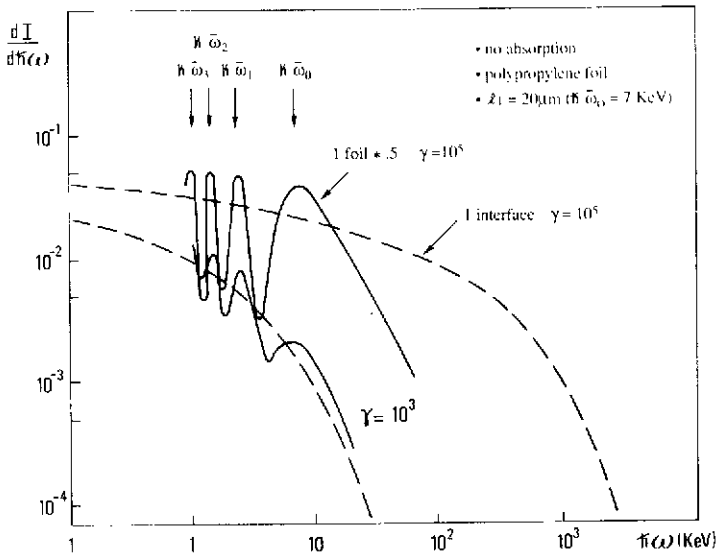

Fig. 6a - Intensity of the forward radiation for 1 foil (* .5) and 1 interface

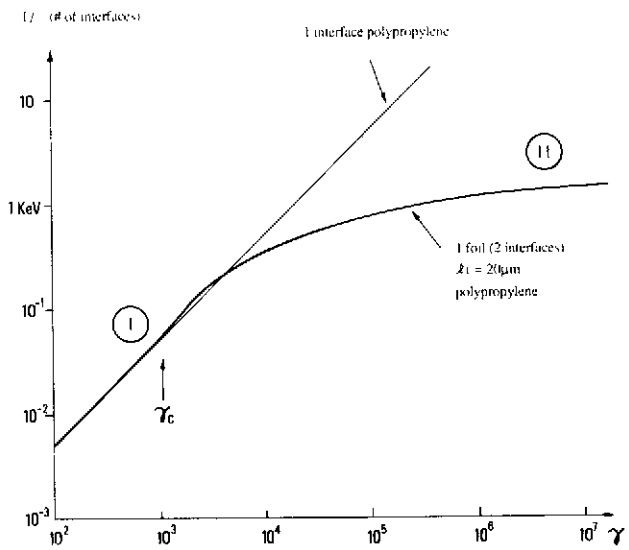

Fig. 6b - Total intensity of the forward radiation divided by the number of interfaces

III.4 - Transition radiation produced by a periodic radiator

We consider now a radiator of N foils of thickness ℓ_1 separated by distances ℓ_2 (ℓ_1 and ℓ_2 are measured along the trajectory of the particle). The plasma frequencies of the foil and gap materials are ω_{p1} and ω_{p2} respectively. Usually we have $\omega \gg \omega_{p1} \gg \omega_{p2}$. The intensity of the forward radiation produced by a unit charge particle crossing the periodic radiator is :

$$\frac{dI}{d\Omega d\hbar\omega}(\text{radiator}) = \frac{dI}{d\Omega d\hbar\omega}(\text{surface}) \cdot F' \qquad (3.8)$$

• F', the multiple interference term is equal to $4e^{-\sigma 1}\, e^{-(N-1)\sigma_{12}}\, F_1\, F_{12N}/F_{12}$

where $F_1 = sh^2(\sigma_1/2) + \sin^2(\varphi_1/2)$ $\quad F_2 = sh^2(\sigma_{12}/2) + \sin^2(\varphi_{12}/2)$

$F_{12N} = sh^2(N\sigma_{12}/2) + \sin^2(N\varphi_{12}/2)$

We have $\varphi_2 = 2\pi\ell_2/Lf_2$ $\quad \sigma_2 = \ell_2/2L_{A2}$ $\quad \varphi_{12} = \varphi_1 + \varphi_2$ $\quad \sigma_{12} = \sigma_1 + \sigma_2$

Lf_2 is the length of the formation zone in the gap material and L_{A2} is the intensity absorption length in this material. The terms F_1 F_{12} and F_{12N} are oscillating, the angular spacing between the oscillations being respectively $\Delta\cos\theta_1 = \lambda/\ell_1$, $\Delta\cos\theta_{12} = \lambda/(\ell_1+\ell_2)$, $\Delta\cos\theta_{12N} = \lambda/N(\ell_1+\ell_2)$. The ratio F_{12N}/F_{12} for large N produces sharp peaks[30-32] with a spacing $\Delta\cos\theta_{12} = \lambda(\ell_1+\ell_2)$.

• For large N we can usually make the approximation $e^{-(N-1)\sigma_{12}}\, F_{12N}/F_{12} = 2\pi\, N_{eff} \sum_m \delta(\varphi_{12}-2m\pi)$ with $N_{eff} = (1 - e^{-2N\sigma_{12}}) / (1 - e^{-2\sigma_{12}})$.

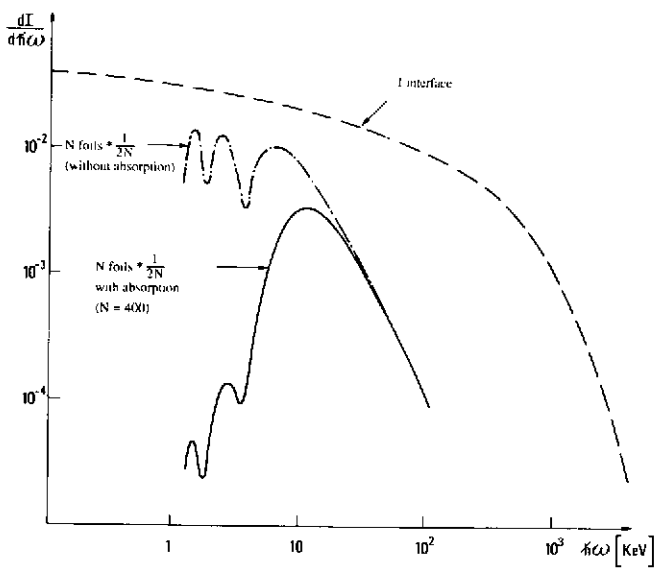

Fig. 7a - Intensity of the forward radiation (divided by the number of interfaces) for $\ell_1 = 20\ \mu m$ $\hbar\omega p_1 = 21$ eV (polypropylene ℓ_2) $= 180\ \mu$ $\hbar\omega p_2 = .27$ eV (helium)

• Using this formula the integration of $dI/d\Omega d\,\hbar\omega$ over angles can be easily done[26] and the differential intensity as a function of $\hbar\omega$ is shown in figure 7a for a typical 8 cm radiator. We note that we still see, neglecting absorption the peaks $\bar{\omega}_0$, $\bar{\omega}_1$, $\bar{\omega}_2$, ... (coming from F_1). If absorption is included only the peak at $\bar{\omega}_0$ stays. Figure 7b shows the intensity per interface for the same radiator.

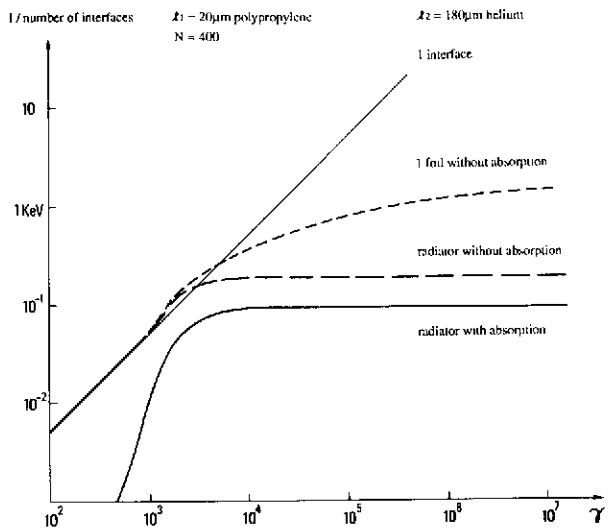

Fig. 7b - Total forward intensity

III.5 - Optimisation of a detector. Miscellaneous

• Generally a transition radiation detector is used in order to sign electrons and reject hadrons (UA2', DØ, H1, ...)[21] but it can also be used in order to sign pions and reject electrons (NA31). In the first case we define the *rejection* $R = \epsilon e / \epsilon \pi$ where $\epsilon \pi$ is the pion contamination and ϵe the efficiency for electrons. R is a function of ϵe via the cuts applied on the measured informations of the n_{ch} chambers.

• The "best" rejection is based on the identification function distribution, by the maximum likelihood principle

$$F = \prod_{i=1}^{n_{ch}} F_i^{\pi} / F_i^{e}$$

where F_i^{π} (F_i^{e}) is the probability that a pion (electron) produces an event with the same information in the chamber # i.

• When we are designing a detector usually the total length D is fixed and we have to optimize all the parameters, the first one being n_{ch} the number of sets (radiator + chamber used for detection of the X-rays) in order to have the best rejection. Doing so we have to take into account the ionisation produced by the charged particle in the chambers and a possible dispersion of ℓ_2 : $\sigma(\ell_2)$[33]. It can be done in a simulation program[34]. As an example the optimisation of the UA2' transition radiation detector for a length D ~ 20 cm gives 2 radiators of 77 mm, each one followed by a Xenon chamber of 23 mm. The dependance of the rejection electron vs pion as a function of other parameters is shown in figure 8[35]. One sees that, for instance the rejection is very sensitive to ℓ_1.

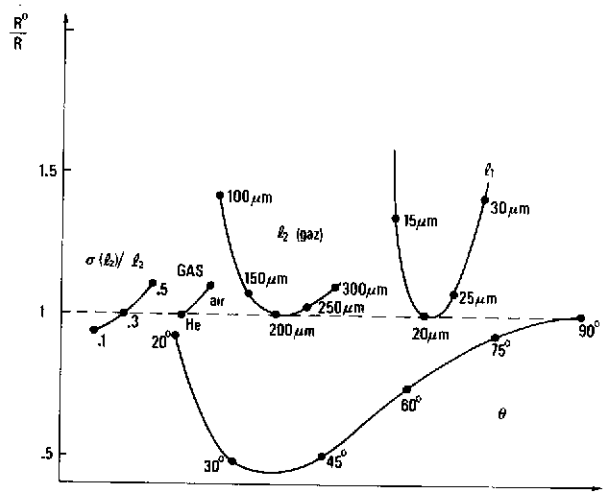

Fig. 8 - Ratio of the (simulated) rejection to pions of the UA2 detector Ro for a standard set of parameters (ℓ_2 = 200 μm, ℓ_1 = 20 μm, θ = 90°, $\sigma(\ell_2)/\ell_2$ = .3, gas = helium) divided by R, rejection for the parameter considered. The rejections are defined at an electron efficiency of 80 %. ℓ_1 and ℓ_2 are the thickness at normal incidence and θ is the incidence angle.

• Flash ADC's are often used in the electronics of the Xenon chamber. We can then have a good knowledge of F^{π} and F^{e} defined above. Unfortunately the gain-using Flash ADC - in rejection is smaller[36] than it was originally[37] thought.

• The X-rays are produced at a finite angle $\theta^{tr} \simeq \omega_p/\omega$. It is unfortunately almost always impossible (see however ref. [38,39]) to detect this finite angle in a non magnetic detector.

• The gas in the chamber is usually mainly Xenon (high Z). For the radiator a low Z material is chosen[40] Li, Be (the best ones) or polypropylene (cheaper and safer).

• The multiple scattering angle in the radiator is approximately given by $\theta d \sim 21/p(MeV)\sqrt{X/Xo}$ where X is the radiation length of the radiator. In the case of UA2' for X/Xo = .017 and p = 10 GeV we have $\theta d \sim 0.2$ mrad $< \theta^{tr} \sim 0.5 \div 1$ mrad.

• Very often e^+e^- conversion pairs are used in detectors in order to test them.
Neglecting the difference of time arrival of the e^+ and e^- the response is proportional to

$$< | 1 - e^{-ikd'} |^2 > = < 2 - 2 \cos \left(\frac{\omega d'}{c} \right) > = < 2 - 2 \cos (2\pi d'/\lambda) >$$

where d' is the difference of the path lengths of the radiations produced by the e^+ and e^-. In the UA2' detector for example the typical separation at the entrance of the radiator of the e^+ and e^- pair produced by a photon of 15 GeV is 70 μm (neglecting multiple scattering) so $d' \sim 70\ \mu m \cdot \theta^{tr} \sim 5\ 10^{-2}\ \mu m$. Since $d' \gg \lambda \sim 6\ 10^{-5}\ \mu m$ we have $< \cos (2\pi d'/\lambda) > \simeq 0$ and the response of the pair is *twice* the response of an electron[41,14].

IV - CONCLUSIONS- FUTURE

Apart from applications described above (beam diagnostics, particle identification) there are other applications of Transition Radiation like the measure of $n(\omega)$[42]. Transition radiation has also been proposed as an X-ray lithography source[27-43]. The next generation of accelerators like LHC and SSC may still use Transition Radiation[21-44] which is good for energies up to more than 200 GeV in addition to calorimetry for electron identification.

ACKNOWLEDGEMENTS

I thank all my colleagues of the Orsay-UA2 group. I also thank X. Artru and L. Wartski for very useful discussions.

REFERENCES

[1] V. Ginzburg and I. Frank, Zh.E.T.P. 16 (1946) 15
(Partial translation in Journal Phys. USSR 9 (1945) 353)

[2] P. Goldsmith and J.V. Jelley, Phil Mag 4 (1959) 836

[3] G.M. Garibyan, Zh.E.T.P. 37 (1959) 527. (Transl. Sov. Phys. JETP 10 (1960) 372)

[4] K.A. Barsukov, Zh.E.T.P. 37 (1959) 1106. (Transl. Sov. Phys. JETP 10 (1960) 787)

[5] I.M. Frank, Nobel lecture 1958, Nobel lectures, Elsevier (1964)

[6] L.C.L. Yuan et al., Phys. Lett. 31B (1970) 603

[7] L. Wartski et al., J. Appl. Phys. 46 (1975) 3644

[8] M.L. Ter-Mikaelian, High Energy Electromagnetic Processes in Condensed Media, Wiley Interscience, New York (1972).

[9] V.L. Ginzburg and V.N. Tsytovich, Phys. Rep. 49 (1979) 1, Phys. Lett. 79A (1980) 16.

[10] I.M. Frank, Usp. Fiz, Nauk 87 (1965) 189. (Transl. Sov. Ph. Usp 8 (1966) 729).

[11] L. Wartski, thèse Université Paris-Sud, Orsay (1976).

[12] J.C. Ashley, Phys. Rev. 155 (1967) 208.

[13] M. Born and E. Wolf, Principles of optics, 3rd edition, Pergamon (1965)

[14] J.D. Jackson, classical electrodynamics, 2nd edition, Wiley (1975)

[15] V. Ginzburg, Physique théorique et astrophysique, Editions Mir (1978)

[16] V. Ginzburg, The lesson of Quantum Theory, p.113, edited by J. de Boer et al., Elsevier (1986)

[17] J. Bosser et al., NIM A238 (1985) 45.

[18] H. Bergeret et al., LAL SERA 87-285

[19] A. Dubrovin, LAL SERA 88-110

[20] R.B. Fiorito et al., European Particle Accelerator Conference, Rome (June 1988)

[21] B. Dolgoshein, NIM A252 (1986) 137

[22] L. Durand, Phys. Rev. D11 (1975) 89

[23] M.L. Cherry et al., Phys. Rev. D10 (1974) 3594

[24] M.L. Cherry, Phys. Rev. D17 (1978) 2245

[25] X. Artru et al., Phys. Rev. D12 (1975) 1289

[26] C.W. Fabjan and W. Struczinski, Phys. Lett. 57B (1975) 483

[27] M.A. Piestrup, IEEE Journ. on Quant. Electr. 24 (1988) 591

[28] G.M. Garibyan, Zh.E.T. 38 (1960) 1814. (Transl. Sov. Phys., JETP 11 (1960) 1306)

[29] P.J. Ebert et al., Phys. Rev. Lett. 54 (1985) 893

[30] M.J. Moran et al., Phys. Rev. Lett. 57 (1986) 1223

[31] G.M. Garibiyan et al., Zh.E.T.P. 66 (1974) 552. (Transl. Sov. Phys. JETP 39 (1974) 265)

[32] F. Feinstein, thèse Université d'Orsay (décembre 1987)

[33] G.M. Garibyan et al., NIM 125 (1975) 133

[34] I. Gavrilenko, private communication

[35] I thank D. Froidevaux for producing this figure

[36] See for instance R.D. Appuhn et al., NIM A263 (1988) 309,
M. Holder and H. Suhr, NIM A263 (1988) 319

[37] T. Ludlam et al., NIM 180 (1981) 413 ; C. Fabjan et al., NIM 185 (1981) 119

[38] A. Alikhanian et al., Phys. Rev. Lett. 25 (1970) 635

[39] M. Deutschmann et al. NIM 180 (1981) 409

[40] W. Willis, Proc. of Intern. Conf. on Trans. Rad. (Erevan 1977)

[41] I thank B. Mansoulié for a useful discussion on this subject

[42] M. Moran, NIM B33 (1988) 18

[43] X. Artru et al., Orsay

[44] T. Akeson et al., CERN 88-02 (April 1988)